

Resonant heavy-ion elastic scattering from s - d shell nuclei

R. Ost, M. R. Clover, R. M. DeVries,* B. R. Fulton, H. E. Gove, and N. J. Rust†

Nuclear Structure Research Laboratory, Rochester, New York 14627

(Received 18 August 1978)

Angular distributions at angles $130^\circ < \theta_{\text{c.m.}} < 180^\circ$ have been measured for $^{12}\text{C} + ^{28}\text{Si}$, ^{32}S , ^{40}Ca as well as ^9Be , $^{13}\text{C} + ^{28}\text{Si}$ in the energy range $20 \text{ MeV} < E_{\text{c.m.}} < 35 \text{ MeV}$. Cross sections rising towards 180° are observed for all reactions. Excitation functions for the back angle enhancement show distinct structures, most pronounced for $^{12}\text{C} + ^{28}\text{Si}$. Angular distributions for ^{12}C , especially those corresponding to peaks in the excitation function show oscillations of the type $P_J^2(\cos\theta)$. The ^{12}C back angle enhancement decreases with target mass. Backscattering of the non- α nuclei ^9Be and ^{13}C is reduced by about two orders of magnitude in comparison with ^{12}C . Standard theoretical approaches fail to explain all the observed effects.

NUCLEAR REACTIONS $^{12}\text{C} + ^{28}\text{Si}$, $^{12}\text{C} + ^{32}\text{S}$, $^{12}\text{C} + ^{40}\text{Ca}$, $^9\text{Be} + ^{28}\text{Si}$, $^{13}\text{C} + ^{28}\text{Si}$,
measured $\sigma(\theta, E)$ elastic scattering, $130^\circ < \theta_{\text{c.m.}} < 180^\circ$, $20 \text{ MeV} < E_{\text{c.m.}} < 35 \text{ MeV}$,
deduced J^π of resonances.

INTRODUCTION

The forward angle scattering of heavy ions is well described by strong absorbing potentials over a wide range of energies.^{1,2} As such potentials predict vanishing back-angle cross sections, until recently no experimental efforts were undertaken to explore the back-angle region. The first such study was reported for $^{16}\text{O} + ^{28}\text{Si}$.³ Surprisingly a strong rise of the elastic scattering cross section towards 180° was observed with an angular distribution of the form $P_J^2(\cos\theta)$, where J equaled the angular momentum of the grazing partial wave. The effect could be well described by several different theoretical approaches.⁴ All these theories failed, however, to describe subsequent back-angle data of ^{12}C , ^{16}O from ^{28}Si .^{5,6} There it was shown that the observations from Ref. 3 do not generally hold. Specifically excitation functions of the back-angle cross sections show resonant behavior. $P_J^2(\cos\theta)$ type angular distributions are only observed for certain energies and in these cases J does not always agree with the angular momentum of the grazing partial wave.

Some indications for these phenomena can be found in earlier publications: Oscillations observed at mid-angles (60° – 120°) cannot be described by simple optical potentials.^{1,2} In the case of $^{16}\text{O} + ^{24}\text{Mg}$ ⁷ resonating excitation functions have been reported for mid-angle cross sections. Back angle enhancements have also been observed for elastic scattering of ^{16}O from ^{20}Ne .^{8,9} Here α -transfer reactions may cause backward-angle oscillations. Calculations on the basis of this assumption, however, do not give satisfying fits to the data. Extensive studies

have been done for the system $^{12}\text{C} + ^{16}\text{O}$.¹⁰ The observed strong resonant behavior of the elastic scattering at back angles in this system is often explained by a set of molecular resonances. This explanation is further supported by the observation of the same resonances in other reaction channels¹¹ and in microscopic predictions.¹² Resonant behavior is well known to occur for scattering of light identical ions ^{12}C and ^{16}O . For a recent review on this subject, see Ref. 13.

Strong enhancements of the elastic back-angle scattering cross section are also well known for the interaction of α particles with α nuclei (this term is used here for nuclei between ^{12}C and ^{40}Ca consisting totally of $2n-2p$ pairs).¹⁴ Although this effect was discovered 20 years ago, there is still no satisfying theoretical description for all its aspects and it has been labeled "anomalous." Excitation functions for anomalous back-angle α scattering can also show strong resonant behavior for many targets (^{20}Ne , Ref. 15; ^{24}Mg , ^{28}Si , Ref. 16).

There exists a multitude of theoretical publications in connection with the anomalous back-angle α scattering, many of which are based on limited experimental results and have not described subsequent measurements. A similar situation arose soon after publication of the first heavy-ion back-angle scattering results.³ This clearly shows the need for more extensive data. It is difficult to take systematic data for α -particle scattering over a wide range of energies as most accelerators only cover a small part of the region of interest. For heavy ions the situation is more favorable. We present here back-angle elastic scattering angular distributions taken at many energies between the Coulomb barrier and the

upper limit of the accelerator for several heavy-ion projectile and target systems.

EXPERIMENTAL METHOD

For all heavy-ion systems studied in this paper, we measured the kinematically reversed reaction (i. e., the heavier of the ions was used as projectile). ^{28}Si (beam currents $\approx 1 \mu\text{A}$), ^{32}S - and ^{40}Ca - ($\sim 100 \text{ nA}$) beams of the University of Rochester MP tandem accelerator were used to bombard carbon and beryllium targets of an approximate thickness of $100 \mu\text{g}/\text{cm}^2$ thus averaging over about $\pm 200 \text{ keV}$ in the center of mass. The elastically scattered carbon and beryllium ions were detected at forward angles corresponding to c. m. angles between 130° and 180° . (We define the heavier particle as target in the c. m. system.) The Enge split-pole, Rochester heavy-ion detector system¹⁷ was used to provide complete mass and charge separation of the detected reaction products. In addition, the system allowed the calculation of the angle of incidence for each incoming particle using the signals from two position wires. This makes it possible to take data for several angles simultaneously. Most of the angular distributions presented here were measured with a 9-slit collimator at the entrance of the spectrograph. An example of the use of this slit is shown in Fig. 1. Counting efficiencies for the different slits were determined by Rutherford scattering of ^{12}C from Au. The mean angle of each slit was calculated from the chamber geometry and from the finite rectangular geometry of the slit. The latter was important for the two smallest angles only. The difference between slits corresponds to a difference in the laboratory scattering angle of 1.17° and the width of one slit to 0.3° (a solid angle of 0.3 msr). Some of the $^{12}\text{C} + ^{28}\text{Si}$ data were taken with only 5 slits of twice-the-above distance and

width. An aluminum foil of thickness $25\text{--}37 \mu\text{m}$ was used to prevent elastic scattered beam particles from entering the detector.

A thin layer of Au ($\sim 0.5 \mu\text{g}/\text{cm}^2$) was evaporated on the targets for normalization purposes. The ratio of C (Be) to Au atoms on the target was determined by Rutherford scattering of a low-energy heavy-ion beam. During the experiment beam particles elastically scattered from Au were detected at 30° in a monitor counter.

A system of three consecutive slits at the entrance of the scattering chamber kept the beam spot ($\sim 1 \times 1 \text{ mm}$) on the target in a stable position. Several runs performed at the beginning and the end of the experiment gave no indication of significant carbon build-up on the target.

To check the accuracy of the absolute normalization, we took data with an ^{16}O beam on the same ^{12}C target used with the ^{28}Si beam. Cross sections for back scattered ^{12}C agree with those reported in Ref. 10. For $E_{\text{c.m.}} = 20.1 \text{ MeV}$ with $^{12}\text{C} + ^{28}\text{Si}$, we measured an angular distribution for the whole angular range $90^\circ\text{--}180^\circ$. Forward angle data taken¹⁸ at the same energy between 0° and 90° show a satisfying connection with our data.

RESULTS

Angular distributions for ^{12}C on ^{28}Si are shown in Fig. 2. In all cases, cross sections rising towards 180° are observed. The magnitude of the backward-angle cross section exceeds the systematic potential² predictions by about 100 at low incident energies and by 10,000 at the higher energies. Most distributions show regular oscillatory behavior and can be well fitted by $P_J^2(\cos\theta)$ with higher J values observed at higher energies. There is no smooth variation of J -values with energy, however. A changeover takes place rather abruptly [as between 24.3 MeV (P_{15}^2) and 24.8 MeV (P_{18}^2)] or is accompanied by irregular non- P_J^2 type angular distributions [as between 30.8 MeV (P_{18}^2) and 33.2 MeV (P_{19}^2)].

We calculated the average cross section in the angular range $155^\circ\text{--}175^\circ$ as a measure of the back-angle enhancement. These values are plotted against energy in Fig. 3. A strongly structured excitation curve is observed with distinct maxima at energies 23.3 , 26.0 , 30.2 , and 33.6 MeV . Comparison with the angular distributions shows that the most regular $P_J^2(\cos\theta)$ type distributions are observed near peaks of the excitation curve, whereas irregular distributions are always to be found at valleys. Note, however, that for the higher energy resonances the envelope of the angular distribution falls off faster than $P_J^2(\cos\theta)$. Therefore, it is likely that more than one process

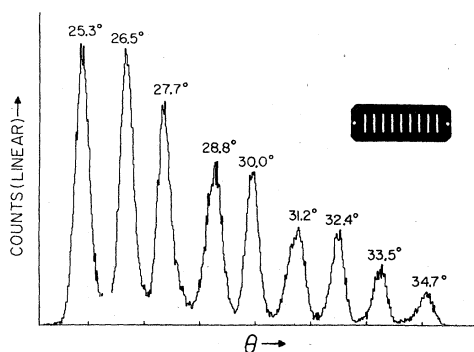


FIG. 1. The 9-slit collimator and resultant angular spectrum.

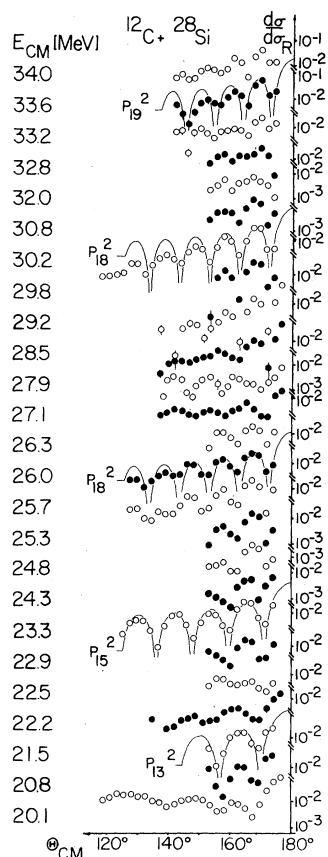


FIG. 2. Sample of elastic angular distributions for $^{12}\text{C} + ^{28}\text{Si}$.

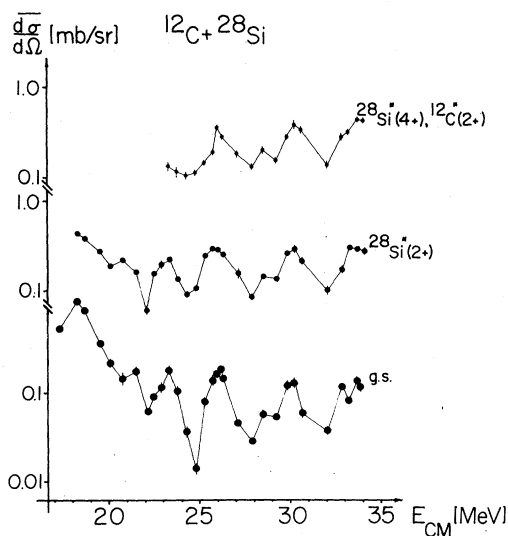


FIG. 3. Excitation functions for back-angle $^{12}\text{C} + ^{28}\text{Si}$ elastic and inelastic scattering. The average back-angle cross sections are calculated over the angular range $155^\circ\text{--}175^\circ$ (g. s.), $157^\circ\text{--}175^\circ$ (^{28}Si 2+), $159^\circ\text{--}175^\circ$ (^{28}Si 4+, ^{12}C 2+).

TABLE I. J values from best $P_J^2(\cos \theta)$ fits to the data (Figs. 2, 5) at peaks of the excitation function ($E_{c.m.}^{\text{res}}$). Fits using a Legendre polynomial of one unit different can be seen in Ref. 5. Values are in brackets if peaks in excitation function are not well defined. The value for l_{gr} , the angular momentum of the grazing partial wave was calculated as discussed in the text.

$E_{c.m.}^{\text{res}}$	J_{obs}	l_{gr}	Reaction
21.5	(13)	15	
23.2	15	17	
26.0	18	19	$^{12}\text{C} + ^{28}\text{Si}$
30.2	18	21	
33.6	(19)	23	
25.8	(12)	18	
28.1	(16)	20	$^{12}\text{C} + ^{32}\text{S}$
29.6	18	21	
32.6	18	23	

is contributing. Furthermore, the fits with $P_J^2(\cos \theta)$ are sometimes ambiguous. For example, the angular distribution at $E_{c.m.} = 33.6$ MeV is fit about equally well with $J=19$ or 20. Therefore, while most of the J assignments are clear, some assignments can only be made to ± 1 unit, depending on the quality of the fit.

J values observed at peaks of the excitation function are listed in Table I together with values for the angular momentum of the grazing partial wave l_{gr} . The values for l_{gr} were calculated using the potential $H12$ —from Ref. 2. However, l_{gr} values calculated with other potentials never differed by more than one unit from those listed in Table I.

The excitation curve is rising towards lower energies. Here we approach the Coulomb barrier where “normal” optical potential scattering is extending into the backward region and interferes

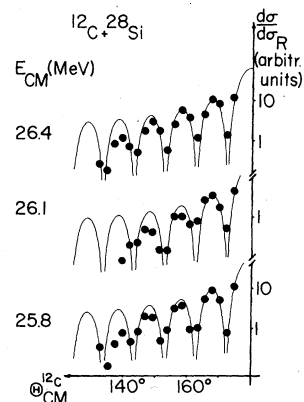


FIG. 4. Elastic angular distributions for $^{12}\text{C} + ^{28}\text{Si}$ measured with a thin target.

with possible resonant behavior.

The excitation curves for inelastic scattering (Fig. 3) to the ^{28}Si 2^+ state at 1.78 MeV, the ^{28}Si 4^+ state at 4.6 MeV and the ^{12}C 2^+ state at 4.43 MeV (the latter two are not resolved experimentally) agree in shape well with the g.s. curve, although the structure is somewhat less pronounced.

Most of the inelastic angular distributions show a near logarithmic rise toward 180° . For the ^{28}Si 2^+ distributions at $E_{\text{c.m.}} = 30.2$ and 33.6 MeV, some structure is visible which allows one to deduce spin values 17 or 18 for $E_{\text{c.m.}} = 30.2$ MeV and 18 or 19 for $E_{\text{c.m.}} = 33.6$ MeV¹⁹ in agreement with J values found for g.s. elastic scattering at these energies.

In Ref. 6, a fine structure was observed for the $^{12}\text{C} + ^{28}\text{Si}$ excitation function at 180° in addition to the gross structure in Fig. 3. This additional structure can not be seen in our experiment as cross sections are averaged over $\Delta E_{\text{c.m.}} \approx 0.4$ MeV due to the energy loss of the Si beam in the carbon target. We performed an additional experiment with a thin carbon target ($\sim 10 \mu\text{g}/\text{cm}^2$) where we measured angular distributions (Fig. 4) at two peaks and one valley for one of the gross structure peaks. Figure 4 shows the same variation in cross section with energy as was observed at 180° .⁶ Notice that at all three energies the same $P_{18}^2(\cos\theta)$ angular distribution is obtained. However, oscillations are more pronounced than those in Fig. 2. Small deviations from perfect $P_{18}^2(\cos\theta)$ distributions are observed, varying for the three energies.

Angular distributions for $^{12}\text{C} + ^{32}\text{S}$ are shown in Fig. 5. The cross sections are reduced in comparison with $^{12}\text{C} + ^{28}\text{Si}$ by about one order of magnitude. $P_J^2(\cos\theta)$ behavior is still observed, with features as discussed for ^{28}Si . However, the oscillations are in general less regular and show a steeper rise towards 180° . The excitation function shows structure, however, much less pronounced than for the ^{28}Si case. There is also less agreement between elastic and inelastic scattering. Observed J values at peaks of the excitation curve are listed in Table I. The discrepancy between J and l_{gr} is similar to ^{28}Si . $^{12}\text{C} + ^{32}\text{S}$ leads to the same compound nucleus (^{44}Ti) as $^{16}\text{O} + ^{28}\text{Si}$. It may therefore be possible to observe the same resonances in both cases. A comparison of our excitation curve (Fig. 6) with the one for $^{16}\text{O} + ^{28}\text{Si}$ (Ref. 6) however shows no similarity at all. In addition, different J values (by about 4 units) are observed at comparable energies for the two reactions.

Two angular distributions have been taken for $^{12}\text{C} + ^{40}\text{Ca}$. Not enough counts were recorded to deduce J values. The overall backward-angle

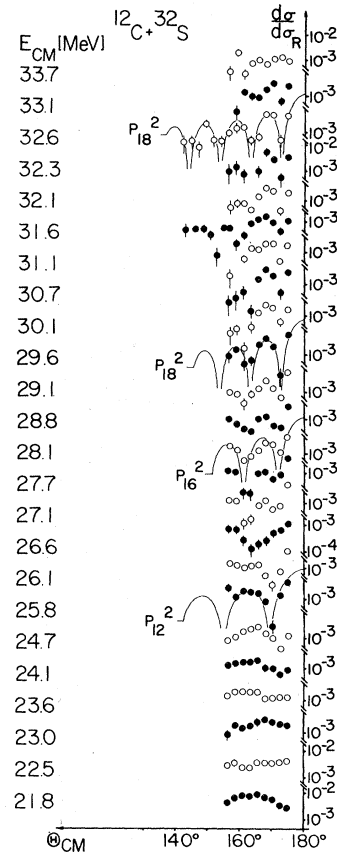


FIG. 5. Elastic angular distributions for $^{12}\text{C} + ^{32}\text{S}$.

cross sections are further reduced and agree with values taken in recent $^{12}\text{C} + ^{40}\text{Ca}$ experiments²⁰ at Brookhaven and Chalk River.

A comparison for backscattering of ^{12}C from different α nuclei is shown in Fig. 7. A drastic reduction of the cross section with target mass is

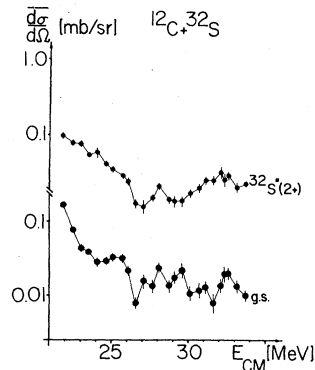


FIG. 6. Excitation functions for back-angle $^{12}\text{C} + ^{32}\text{S}$ elastic and inelastic scattering. The average back-angle cross sections are calculated over the angular range 155° – 175° (g.s.) and 157° – 175° (^{32}S 2^+).

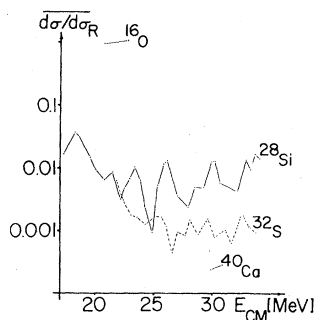


FIG. 7. Comparison of elastic back-angle scattering for ^{16}O , ^{28}Si , ^{32}S , and ^{40}Ca . Values of $d\sigma/d\sigma_R$ are averaged over the angular range 155° – 175° .

observed.

To check whether enhanced back-angle scattering cross sections are restricted to interactions between α nuclei, we also took data for ^9Be ($E_{\text{c.m.}} = 24.1$ MeV) and ^{13}C on ^{28}Si . In both cases, cross sections are nearly two orders of magnitude lower than for $^{12}\text{C} + ^{28}\text{Si}$. The angular distributions (Fig. 8) show a rather featureless rise towards 180° . Cross sections for inelastic scattering and the (^{13}C , ^{12}C) reactions were also measured.

Ground state elastic scattering shows some structure in the excitation curve (Fig. 9) less pronounced however than in the case $^{12}\text{C} + ^{28}\text{Si}$. The peak at $E_{\text{c.m.}} = 26.0$ MeV coincides with a peak of Fig. 3, however at higher energies the excitation curve disagrees with the one for $^{12}\text{C} + ^{28}\text{Si}$. A strong reduction of the back angle enhancement has recently also been observed for $^{18}\text{O} + ^{28}\text{Si}$ compared

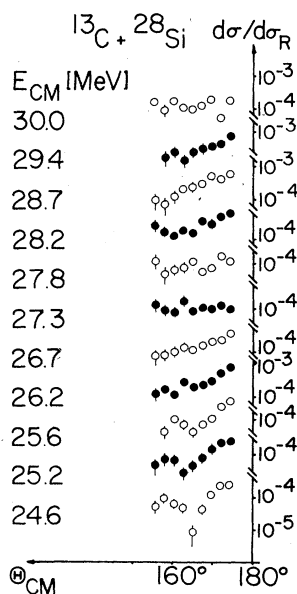


FIG. 8. Elastic angular distributions for $^{13}\text{C} + ^{28}\text{Si}$.

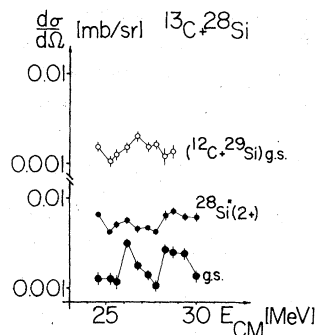


FIG. 9. Excitation functions for back-angle $^{13}\text{C} + ^{28}\text{Si}$ elastic and inelastic scattering and the ^{28}Si (^{13}C , ^{12}C) ^{29}Si reaction. The average back-angle cross sections are averaged over the angular range 155° – 175° (g. s.) and 157° – 175° [^{28}Si 2+ and (^{13}C , ^{12}C)].

with $^{16}\text{O} + ^{28}\text{Si}$.²¹ In contrast to ^{12}C data, the ^{13}C back-angle scattering data can be fitted by only slightly modifying optical model potentials that fit forward data of similar systems.^{1,2}

DISCUSSION AND SUMMARY

There are two basic theoretical approaches to data: (1) We may try to incorporate the process in direct reaction models (optical model and DWBA) that have successfully been used to describe forward-angle data.^{1,2} Clearly, modifications of these models are necessary. (2) We may consider the process as an isolated phenomenon.

The observed resonant structure suggests the involvement of a set of high spin states (molecular resonances) in the corresponding compound nuclei.

The first approach amounts to finding a potential description for the data since the transfer of a massive number of nucleons seems to be ruled out.²² This has recently been achieved successfully for $^{16}\text{O} + ^{28}\text{Si}$. Surface transparent, weakly absorbing potentials have been used²³ to describe the complete angular distribution of Ref. 3. A weak absorption in the surface makes it possible for partial waves near l_{gr} to be scattered in the background hemisphere producing regular $P_l^2(\cos\theta)$ angular distributions with $J = l_{\text{gr}}$. Such a description does not explain the strongly structured excitation curve. It has been shown, however, that multiplication by a parity dependent factor²⁴ [which adds 5 free parameters including an exponential energy dependence in the imaginary potential], introduces a regular up and down movement of the back-angle enhancement with energy. As the excitation curve for $^{16}\text{O} + ^{28}\text{Si}$ ⁶

shows a regular peak to peak distance of ≈ 2.2 MeV a good fit to the data is achieved.

There are two basic differences for ^{12}C elastic back-angle scattering: (1) The grazing partial wave is *not* observed at back angles. (2) Peaks of the excitation function are *not* regularly spaced ($\Delta E = 1.7, 2.8, 4.2, 3.4$ MeV). At back angles enhancement of the cross section is easily achieved for ^{12}C by use of a potential similar to the one in Ref. 23. For some of our data on ^{28}Si forward data¹⁸ are available for comparison. Good fits to the forward region yield the wrong $P_J^2(\cos\theta)$ oscillations at back angles. We were unable to find an acceptable fit to both forward and backward regions of the angular distributions. The situation is still worse if we try to fit the energy dependence of the process. It is clear from the data that a highly energy dependent potential would be required to fit the excitation function. We have applied the parity dependent potential of Dehnhard *et al.*²⁴ to the $^{12}\text{C} + ^{28}\text{Si}$ system with the result that evenly spaced peaks and valleys are predicted in disagreement with our data. It is possible that further patches on the optical model could fit our data, however, we have no such description at this time. Thus, we have to consider the back-angle scattering of ^{12}C as an isolated phenomenon (i.e., separate from direct reaction theory).

The observed structure in the excitation curves is too pronounced and peaks are too wide for an explanation by statistical fluctuations. (The additional fine structure reported in Ref. 6 has recently been explained in this way²⁵ which is consistent with Fig. 4. We then consider the possibility that we are dealing with a set of resonant states with excitation energies and widths as observed in the excitation curves and that the background elastic scattering is described by a "normal" optical potential like $H12$ from Ref. 2. Multiplying the elastic scattering S matrix with a set of Breit-Wigner terms for resonances of the observed width and energy gives a good description of the angular distributions measured at peaks of the excitation curves.²⁶ In valleys, however, the method fails to describe the data. Here an improved optical model description of the elastic scattering background and the inclusion of additional hidden resonances may be necessary.

Level densities at corresponding excitation en-

ergies in the compound nucleus differ by more than one order of magnitude for α nuclei and non- α nuclei. This may explain the observed differences between ^{12}C and ^{13}C back-angle scattering. For ^{12}C , few levels are available for l values close to l_{gr} which may be the cause of the resonances observed for $^{12}\text{C} + ^{28}\text{Si}$. For $^{13}\text{C} + ^{28}\text{Si}$, on the other hand, the compound nucleus level density is much higher which may explain the weakness of resonant structure in the excitation function.

There are, however, aspects of the data that do not agree with a picture of resonant molecular states. We would expect such states to fall on a rotational band. This is in contrast to the unusual spin sequences observed (Table I).

The best known example for molecular resonances is the system $^{12}\text{C} + ^{12}\text{C}$, where the same excitation structure has also been observed for various reactions (including fusion) leading to ^{24}Mg .¹³ For $^{12}\text{C} + ^{28}\text{Si}$, ^{32}S correlated structure is only observed for elastic and inelastic scattering (with poor correlation for ^{32}S). No structure is observed for fusion.²⁷ As mentioned earlier, the systems $^{12}\text{C} + ^{32}\text{S}$ and $^{16}\text{O} + ^{28}\text{Si}$, which form the same compound nucleus, do not show any correlation in their back-angle elastic scattering. Similar observations have been made comparing the systems $^{16}\text{O} + ^{16}\text{O}$ and $^{12}\text{C} + ^{20}\text{Ne}$.²⁸

Excitation functions for the α -transfer reaction $^{24}\text{Mg}(^{16}\text{O}, ^{12}\text{C})^{28}\text{Si}$ have been measured recently.²⁹ For this case some back-angle elastic data are available in both entrance³⁰ and exit channel. We would expect the excitation curve of the α transfer to show the structure of either entrance or exit channel or a mixture of both. No clear correlations are observed, however.

To summarize the present situation: For interactions between α nuclei, oscillating enhanced back-angle elastic scattering cross sections are observed. The back-angle enhancement shows strongly structured excitation curves. Neither standard direct or compound theories nor molecular resonances so far give a general description of the observed effects.

We would like to thank R. Cherry, Jr., and N. Anantaraman for their help with part of the data taking.

*Permanent address: MS456, LASL, Los Alamos, New Mexico 87545.

†Permanent address: Physics Department, University of Stellenbosch, Stellenbosch 7600, South Africa.

¹J. G. Cramer, R. M. DeVries, D. A. Goldberg,

M. S. Zisman, and C. F. Maguire, Phys. Rev. C **14**, 2158 (1976).

²R. M. DeVries, D. A. Goldberg, J. W. Watson, M. S. Zisman, and J. G. Cramer, Phys. Rev. Lett. **39**, 450 (1977).

- ³P. Braun-Munzinger, G. M. Berkowitz, T. M. Cormier, C. M. Jachcinski, J. W. Harris, J. Barrette, and M. J. LeVine, *Phys. Rev. Lett.* **38**, 944 (1977).
- ⁴Proceedings of the Symposium on Heavy Ion Elastic Scattering, University of Rochester, 1977 (unpublished).
- ⁵M. R. Clover, R. M. DeVries, R. Ost, N. J. A. Rust, R. N. Cherry, Jr., and H. E. Gove, *Phys. Rev. Lett.* **40**, 1008 (1978).
- ⁶J. Barrette, M. J. LeVine, P. Braun-Munzinger, G. M. Berkowitz, M. Gai, J. W. Harris, and C. M. Jachcinski, *Phys. Rev. Lett.* **40**, 445 (1978).
- ⁷W. Mittig, P. Charles, S. M. Lee, I. Badaway, B. Berthier, B. Fernandez, and J. Gastebois, *Nucl. Phys.* **A233**, 48 (1974).
- ⁸R. Vandenbosch, M. P. Webb, and M. S. Zisman, University of Washington, Annual Report, 1975, Seattle, WA (unpublished).
- ⁹R. Stock, U. Jahnke, D. L. Hendrie, J. Mahoney, C. F. Maguire, W. F. W. Schneider, D. K. Scott, and G. Wolschin, *Phys. Rev. C* **14**, 1824 (1976).
- ¹⁰P. Charles, F. Auger, I. Badaway, B. Berthier, M. Dost, J. Gastebois, B. Fernandez, S. M. Lee, and E. Plagnol, *Phys. Lett.* **62B**, 289 (1976), and references therein.
- ¹¹D. Shapira, R. M. DeVries, M. R. Clover, R. N. Boyd, and R. N. Cherry, Jr., *Phys. Rev. Lett.* **40**, 371 (1978), and references therein.
- ¹²D. Baye and P. H. Heenen, *Nucl. Phys.* **A283**, 176 (1977).
- ¹³D. A. Bromley, in *Proceedings of the Second International Conference on Clustering Phenomena in Nuclei*, College Park, Maryland, 1975, edited by D. A. Goldberg, J. B. Marion, and S. J. Wallace [U.S.E.R.D.A. (Technical Information Center), Washington, D.C., 1975].
- ¹⁴J. S. Eck, W. J. Thompson, K. A. Eberhard, J. Schiele, and W. Trombick, *Nucl. Phys.* **A255**, 157 (1975), and references therein.
- ¹⁵A. A. Cowley, J. C. van Staden, S. J. Mills, P. M. Cronje, G. Heymann, and G. F. Burdzik, *Nucl. Phys.* **A301**, 429 (1978).
- ¹⁶A. Budzanowski, K. Grotowski, and A. Strzalkowski, in *Proceedings of the Second International Conference on Clustering Phenomena in Nuclei*, University of Maryland, College Park, Maryland, 1975, Ref. 13.
- ¹⁷D. Shapira, R. M. DeVries, H. W. Fulbright, J. Toke, and M. R. Clover, *Nucl. Instrum. Methods* **129**, 123 (1975).
- ¹⁸C. M. Cheng, J. V. Maher, W. Oelert, and F. D. Snyder (unpublished).
- ¹⁹We thank D. Shapira who deduced these spin values for us with his computer program PAZIT.
- ²⁰S. Kubono, P. D. Bond, C. E. Thorn, and M. J. LeVine, *Bull. Am. Phys. Soc.* **23**, 615 (1978), and private communication; T. Renner, D. Horn, G. C. Ball, W. G. Davies, and J. P. Schiffer, Chalk River National Laboratory, Annual Report, 1977 (unpublished), p. 21.
- ²¹P. Braun-Munzinger and J. Barrette, in Symposium on Heavy Ion Elastic Scattering (see Ref. 4), p. 85.
- ²²M. S. Zisman, in Symposium on Heavy Ion Elastic Scattering, (see Ref. 4), p. 473.
- ²³V. Shkolnik, D. Dehnhard, S. Kubono, M. A. Franey, and S. Tripp, *Phys. Lett.* **74B**, 195 (1978); E. H. Auerbach, A. J. Baltz, M. Golin, and S. H. Kahana, Symposium on Heavy Ion Elastic Scattering (see Ref. 4), p. 394.
- ²⁴D. Dehnhard, V. Shkolnik, and M. A. Franey, *Phys. Rev. Lett.* **40**, 1549 (1978).
- ²⁵J. Barrette, M. J. LeVine, P. Braun-Munzinger, G. M. Berkowitz, M. Gai, J. W. Harris, C. M. Jachcinski, and C. D. Uhlhorn, *Bull. Am. Phys. Soc.* **23**, 615 (1978).
- ²⁶M. R. Clover, Ph.D. thesis, The University of Rochester, 1978 (unpublished).
- ²⁷R. Ost, M. R. Clover, B. Fulton, and B. Sikora (unpublished).
- ²⁸R. Vandenbosch, M. P. Webb, and M. S. Zisman, *Phys. Rev. Lett.* **33**, 842 (1974); H. Doubre, J. C. Roynette, E. Plagnol, J. M. Loiseaux, P. Martin, and P. deSaintignon, *Phys. Rev. C* **17**, 131 (1978).
- ²⁹M. Paul, S. J. Sanders, J. Cseh, D. F. Geesaman, W. Henning, D. G. Kovar, C. Olmer, and J. P. Schiffer, *Phys. Rev. Lett.* **48**, 1310 (1978).
- ³⁰S. M. Lee, J. C. Adloff, P. Chevallier, D. Disdier, V. Rauch, and F. Scheibling, in *Third International Conference on Clustering Aspects of Nuclear Reactions Manitoba, 1978*, edited by W. T. H. van Oers, J. P. Svenne, J. S. C. McKee, and W. R. Falk (AIP, New York, 1978).